Experiment investigation of heat transfer in a rotating lateral outflow trapezoidal channel with pin-fins under high rotation numbers and Reynolds numbers

Xuejiao Zhang[a,b], Haiwang Li[a,b], Ruquan You[a,b,*],
Song Liu[a,c], Zhi Tao[a,b]

[a] Research Institute of Aero-Engine, Beihang University, Beijing, 100191, China

[b] National Key Laboratory of Science and Technology on Aero Engines Aero-thermodynamics, Beihang University, Beijing, 100191, China

[c] AECC Sichuan Gas Turbine Establishment

***Corresponding Author: youruquan10353@buaa.edu.cn**

ABSTRACT

In this study, the heat transfer characteristics in a rotating lateral outflow trapezoidal channel with pin fins, which is a typical model of the internal cooling passage in a turbine blade, were experimentally investigated under the Reynolds number range of 10,000 – 80,000, rotating speed range of 0 – 1000 r/min. The tested Re and Ro ranges are considerably extended from the previous experiences. For the non-rotating condition, the heat transfer characteristics of the leading and trailing sides of the internal channel are relatively uniform, whereas there are variations for the leading and trailing sides of the outer side. On the inner smooth surface, at Re=30000 of non-rotating., the leading and trailing averaged Nusselt number of the point near the inlet is about 48% higher than that at the end of the channel, but on the outer pin-fin arrayed surface, the averaged Nusselt number decreases about 20.5%. For the rotating conditions, the heat transfer of inner leading surface significantly reduced due to the rotation-induced Coriolis force and coolant discharged from the channel along the side outlets. Interestingly, with Reynolds number increases, the Nusselt number ratios decreases. When the rotating speed is 1000 r/min and the Reynolds number is 10000, 3000, 50000 and 70000, the Nusselt number ratios are 2.11, 1.40, 1.19 and 1.07 respectively. Moreover, the leading side of the inner smooth area exhibit a critical rotation number, in which the rotation weakened the heat transfer before the critical point and promoted heat transfer after the critical point. However, the critical rotation number varied with X/D.

Keywords: rotating lateral outflow channel, trailing edge, pin-fins, heat transfer.

1.Introduction

At present, the temperature in front of advanced Aero-engine Turbine reaches 1500 ℃ ~ 1700 ℃, while the temperature resistance of turbine blade material is about 1100 ℃. Therefore, an effective cooling method must be adopted to cool the turbine blade so that it can work continuously and stably. Turbine blade cooling technology can be divided into two categories: external film cooling and thermal barrier coating technology, and internal enhanced cooling air and blade surface heat exchange technology. Internal cooling scheme, the leading edge often adopts impingement jet cooling, the middle serpentine ribbed channel to increase the heat exchange area, and the pin fins is used to cool the trailing edge which is difficult to cool, and effectively improves the support strength of this area [1].

Non-inertial forces will be generated in the rotating cooling channel: rotating centrifugal force and Coriolis force; The combined action of centrifugal force field and temperature field induce Buoyancy[2]. These additional forces act on the flow and heat transfer in the channel, and the Coriolis force has the most significant effect on the heat transfer. Fu et al. [3] examined the effect of buoyancy parameter double rectangular rotating channel on heat transfer, the results show that increasing the local buoyancy parameter will increase the Nusselt number ratio on the trailing surface and decreases on the leading surface at the first passage. Li et al. [4] For the leading and trailing surfaces, there is a critical buoyancy value at each X/ D position. Under the condition of high rotation number, strong buoyancy effect is useful to enhance heat transfer. Wagner et al. [5] analyzed the effect of buoyancy and Coriolis， the heat transfer coefficients increase by 250% under no rotation. Liu et al. [6] investigated that the rotation and buoyancy numbers can predict used to determine the extent of increase in the heat transfer.

Lateral outflow is an important characteristic of turbine blade trailing edge cooling structure. The research of this part needs to consider not only the heat transfer in the channel, but also the external flow and heat transfer, which is usually difficult. Liu et al. [7] researched wedge-shaped cooling channel with slot ejection, the slot jet produces turbulent mixing in the narrow region, and the rotation effect in the slot region is less than that in the wide region of the wedge channel. The average heat transfer enhancement of slot ejection is higher than that of non-slot ejection. Hwang et al. [8] founded that for a single outlet channel, the mean Nusselt number of the wedge-shaped channel with lateral outflow of the pin-fins is sensitive to the arrangement of the pin-fins, which heat transfer is higher than the corresponding pin array in the straight outlet channel. Tao et al. [9]

experimentally studied smooth wedge-shaped channel with lateral outflow, according to the experimental data, the outlet boundary conditions affect the heat transfer in non-rotating state, but have little effect at high speed. Deng et al.[10] reported the heat transfer of double inlet side outlet wedge channel, with the increase of flow coefficient, the heat transfer at the top-half increases, but the heat transfer at the bottom-half decreases, and the worst heat transfer is obtained when the flow coefficient is 0.55.

In gas turbine engines, pin-fins are widely used to cool the trailing edge of gas turbine vanes blade, and an array of pin-fins is used rather than a single pin-fin. The flow in the channel with pin fins is very complex and has strong three-dimensional characteristics. Wright et al. [11] studied the heat transfer characteristics of wedge-shaped channel with pin fins, the maximum heat transfer coefficient is near the slot, which significant enhances the heat transfer compared with the smooth channel. Metzger et al. [12] designed a channel models with circular cross-section pin-fins, the experimental results showed that the heat transfer coefficient of the pin-fins surface is about twice of the end wall of the channel. Facchini et al.[13] recommended a wedge-shaped channel with an insert to consider the influence of accelerated flow， compared with the previous studies in the constant height channel with pin-fins, the Reynolds number is only slightly reduced, and the heat transfer value of the pin-fins is 2.3 times that of the end-wall surface.

Chyu et al. [14] indicated that cube element always produces the highest heat transfer, followed by diamond and pin-fins. In addition, for a given shape, staggered arrays usually have greater heat transfer enhancement and pressure loss than the corresponding linear arrays. Hwang and Lu [15] confirmed that the heat transfer enhancement of square, diamond and circular pins is about 170 - 260%, 160 - 260% and 130 - 210% respectively compared with the fully developed smooth channel results. Liang et al. [16] recommended the wedge-shaped channel of the guiding pin fin arrays is studied. Compared with the baseline circular pin-fins array, the Nusselt number of the guiding pin-fins array is significant improved, the total Nusselt number increased by 11.5% - 13.8%. Goldstein and Chen [17] investigated a uniform-diameter circular pin-fins (UDFC) and two stepped diameter circular pin-fins (SDCF1 and SDCF2) are studied. The near end-wall flow changes row by row until the third row reaches a stable mode, and SDCF2 array has the highest mass transfer rate, SDCF1 array has the smallest pressure loss. Uzol and Camci [18] indicated that the wall heat transfer enhancement capacity of circular pin-fin array is 25 - 30% higher than that of elliptical pin fin array, and the pressure loss produced by circular pin fin array is 100 - 200% higher than that of elliptical pin fin array.

Flow separation and laminar turbulence transition will occur on each pin-fin, which leads to the sensitivity of heat transfer coefficient to the arrangement of pin-fins. Dhumne [19] indicated that the length diameter ratio of the pin-fins is the main factor affecting the heat transfer level of the channel. A lower spacing ratio of the pin-fins is conducive to improve the heat transfer capacity. Brigham and Vanfossen [20] experimented eight row and four row staggered pin-fins structure (length to diameter ratio of 4), the heat transfer is higher than that in similar on shorter pin-fins (length to diameter ratio of 1/2 and 2). In addition, for the pin-fins structure with length to diameter ratio of 4, the average heat transfer of the eight rows staggered pin-fins array is slightly higher than that of only four rows.Pascotto et al. [21] numerically studied the influence of rotation on the flow field in the trailing edge cooling channel, changing the orientation will attenuate the influence of rotation on the inlet and top area of the channel. Qiu et al. [22] compared the effect of channel direction on heat transfer in rotating wedge cooling channel is studied. There is an obvious critical rotation number in 180 ° and 135 ° configurations. After the critical rotation number, the heat transfer properties will suddenly change, but not under 90 ° one. Srinivasan et al. [23] numerically calculated the heat transfer in wedge-shaped trailing edge channel. When the orientation angle changes from 180 ° to 90 ° at an interval of 45 °, the Nusselt number ratio changes little in the first half (180 ° - 135 °), but it changes significantly in the second half (135 ° - 90 °). Currently, the flow and heat transfer in the channel are more sensitive to the channel orientation. Willett and Bergles [24] noted that compared with the case of 90 ° channel orientation, the heat transfer of the leading edge in the radial outlet channel with 150 ° channel orientation is strengthened. But in general, the average heat transfer efficiency of the whole channel decreases, and the rotation orientation weakens the influence of rotation.

In addition to the above about the channel and pin-fins structure, the influence of boundary conditions on heat transfer intensity is very important. Han et al. [25] analyzed the effect of uneven wall temperature on the heat transfer coefficient of smooth rotating double square channel ， and uneven wall temperature on the heat transfer coefficient of the second channel is greater than that of the first channel. Han et al. [26] recommended that the local wall heating condition produces local buoyancy, which reduces the influence of bulk buoyancy and Coriolis force， and changes the local heat transfer coefficient of the leading and trailing surfaces. Bai et al. [27] investigated the heat transfer characteristics of a rectangular channel with multiple inlets and outlets, a critical mass ratio existed in the central region.

In conclusion, the characteristics of

turbine blade trailing edge cooling structure are: high aspect ratio cross section, pin-fins array, large channel orientation and lateral outflow. Therefore, the effect of heat transfer on the rotation of trailing edge channel should be studied. The existing heat transfer research of wedge-shaped channel with needle fin at the trailing edge mainly focuses on the case that the Reynolds number is less than 40000. Therefore, the study rarely involves large inlet parameters, resulting in uncertainty in this regard. In this study, a wedge-shaped trailing edge with needle fins was developed for high Reynolds number (80000) and rotating speed (1000 r/min). The heat transfer differences under different inlet conditions are compared.

Naming rules

English symbols

A	copper plate area (m2)
Buo	buoyancy number
Dh	channel hydraulic diameter (m)
h	convective heat transfer coefficient (W/ (m2 · K))
I	current of heater (A)
$\dot{m}$	mass flow rate (kg/s)
Nu	Nusselt number
P	measured point in radial direction
Q	heat transfer rate (W)
r	distance from the center of rotation to the inlet (m)
R	resistance of a film heater (Ω)
Re	Reynolds number
Ro	rotation number
T	temperature (K)
TR	wall-to-fluid temperature ratio
U	mean inlet velocity (m/s)
X	coordinate in radial direction (m)

Greek symbols

α	heat-loss coefficient (W/K)
μ	dynamic viscosity coefficient of air (Pa · s)
ρ	density of the coolant (kg/m3)
Ω	

Subscripts

ave	averaged parameter
b	bulk temperature

e	environment
i	index of the measured point
in	inlet
loss	loss
net	net
out	outlet
S	stationary
w	wall
X	local parameter

2.Experimental setup

2.1. Rotating facility

As shown in Fig. 1, rotating facility includes the following modules. A motor with power of 132kW DC to directly drive the rotating shaft, it can achieve continuous speed changes from 0 to 2500r/min. The diameter of rotating disk is 0.9m mounted on the rotating shaft. Vibration sensors are installed on each axis in the both horizontal and vertical directions to monitor abnormal vibration of the rotating shaft. The pressurized air supply system realizes compressed gas converse dynamic into static, gas pressure ranges from 0.1MPa to 0.8 MPa, and the maximum Reynolds number that exceeds 110000. The compressed coolants supplied to the test section and gas at the outlet of the channel are regulated with two independent mass flow meters. Temperature and pressure signals measured by 12 Adams, which can measure 96 signals. Eight-channel slip ring to switch the analogue signals of the thermocouples and pressure sensor to digital ones. Two Control valves installed in inlet and outlet pipelines to adjust flow rate and pressure for the experiment.

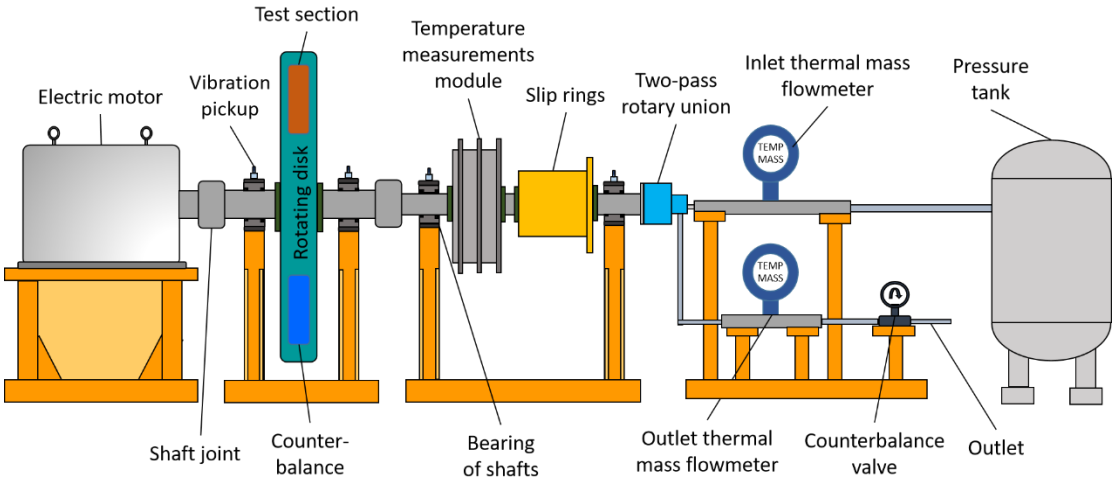

Figure 1. Rotating facility.

2.2. Experimental piece

As shown in Fig. 2, the test section is a single-inlet wedge-shaped lateral outflow channel with 6 arrays pin-fins. The cross-section of the channel is a trapezoid with height of 19mm, and the height of other models is 22mm. The length of lateral outflow is 60mm. Other geometric dimensions of the experimental model are shown in the figure 2 , experimental model parameters used in the study are shown in table 1. The material of the fin-pins is titanium alloy. The copper plates temperature measuring points are assembled in a Nylon skeleton on walls to measure the averaged convection heat transfer coefficient. The pin-fins are glued onto the Nylon skeleton and heated copper plates.

Copper plates are embedded in a nylon skeleton and fixed with quick-drying glue. It should be noted that, as with Fig. 3, the leading and trailing surface structure of pin fin area copper plates are dissimilar. The copper plates installed at the leading surface has many through holes for installing the pin fins. A film heater is glued on the back of each copper plate to supply steady heat flux. The temperature of copper plate is measured by thermocouples installed in the reserved hole on the back of the copper plates. The temperature represents the average temperature of the copper, since its Bivolt number is far less than 0.1. The fluid temperatures of two inlets and eight side-wall slots are also measured. Four thermocouple and two pressure measure are arranged at both inlet and outlet of the channel, fluid temperatures and pressure of inlets and outlet are measured. A length of 60mm unheated entrance is added before the entrance of the channel. Before inlet is equipped with a honeycomb structure to provide a stable airflow. The gas discharged from the outlet is directly discharged into the pressurized vessel. A pressure regulator valve is employed after outlet mass flowmeter to adjust the back pressure.

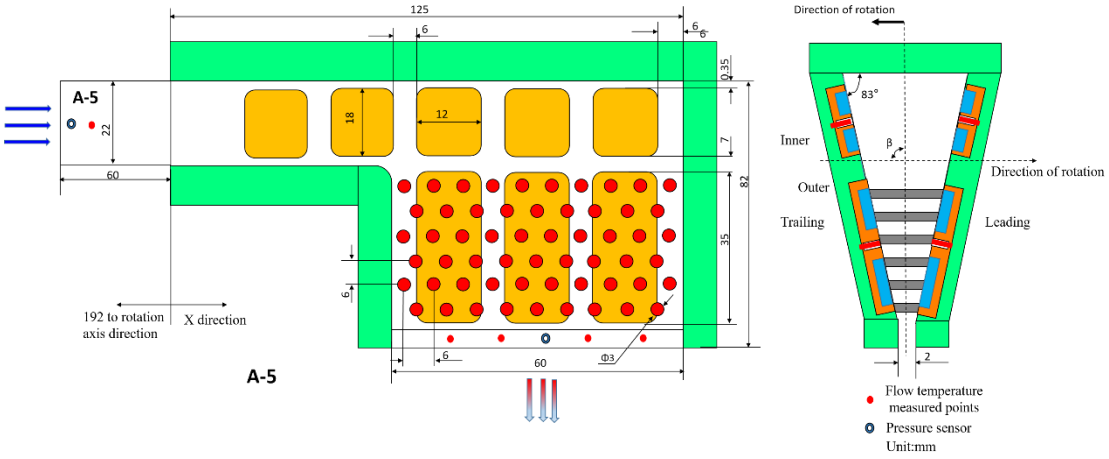

Fig. 2. The diagram of the test section.

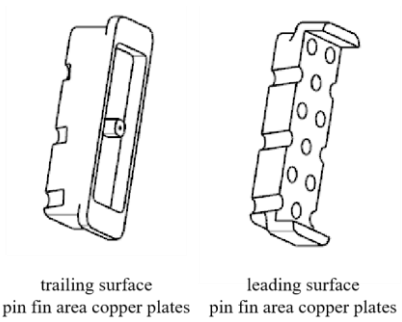

Fig. 3. The diagram of pin fin area copper plates

As shown in Fig. 4, in the span-wise, the regions which smoothly are marked as "inner", while the parts arranged with pin fins are named as "outer". Identically, the numbers outside brackets represent the copper plates at the leading surface, trailing ones are in brackets. The experimental parameters are summarized in Table 2.

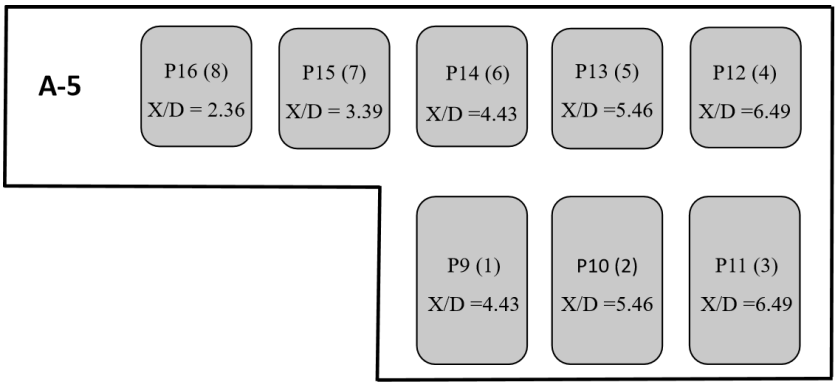

Fig. 4. The diagram of measuring points

Table 1

Experimental model parameters used in the study.

Parameter	Dh (mm)	d (mm)	S_X/d	S_Y/d	r/Dh	Number of pins	X/Dh
A-5	17.4	3	6	6	11.03	67	2.23 (P16/P8), 3.39 (P15 /P7), 4.43 (P14 /P6/P9/P1), 5.46 (P13/P5/P10/P2), 6.49 (P12/P4/P11/P3),

Table 2
Experimental parameters used in the study

Parameter	Values
Re	10,000– 80,000
n	0–1000 r/min
TR	0.14
β	90°
Back pressure	Approximately 5 atm
A_{in}	319.44mm^2

3. Data reduction

T The data derivation for a rotating heat transfer has been introduced in several articles. Because the Bivolt number of each copper plate is less than 0.1, the temperature variation on each copper plate can be neglected. Therefore, the local convective heat transfer coefficient can be calculated as follows:

$$h_i = \frac{Q_{net,i}}{(T_{w,i}-T_{b,i})A_{cu,i}} = \frac{I^2R_i-Q_{loss,i}}{(T_{w,i}-T_{b,i})A_{cu,i}},$$

where $T_{w,i}$ is the local wall temperature of the channel (temperature of the copper plate measurement point), $T_{b,i}$ is the average temperature of the local main stream, $A_{cu,i}$ is the heat exchange area of a single copper block, I^2R_i is the heating power of a single heating film, and $Q_{loss,i}$ is the heat loss of a single copper block.

For the heat loss of copper, a one-dimensional heat-loss coefficient is used; the relationship between the heat dissipation of the copper plates and the environment should be established. In this study, the heat dissipation of the copper plates to the environment was considered, whereas the wall temperature of the copper plates in the flow and span-wise directions was ignored. The heat-loss coefficient (Q_{loss}) can be defined as follows:

$$\alpha_i = \frac{Q_{loss}}{T_{w,i}-T_e} = \frac{I^2R_i}{T_{w,i}-T_e} = f(\Omega).$$

Therefore,

$$Q_{loss,i} = \alpha_i(T_{w,i} - T_e).$$

Accordingly, the local Nusselt number on the wall can be calculated using

$$Nu_i = \frac{h_iD_h}{\lambda},$$

where λ is the thermal conductivity of the gas calculated as:

$$\lambda\ (T) = 2.456 \times 10^{-4}T^{0.823}.$$

4. Results and discussions

4.1 Heat transfer distributions in the non-rotating channels

Before study the rotation effects on heat transfers, it was vital to verify the non-rotation results and set them as references. Fig. 4(a) illustrates the span-wise Nusselt number distributions at different Reynolds numbers, whereas Fig. 4 (b) shows the averaged Nusselt number ratio variation under four major inlet Reynolds number cases. Due to the geometry of the inner region of the

channel is symmetrical, the heat transfer difference between the leading and trailing surfaces is very limited. However, the copper block at the leading surface of the external area in the channel has pin fin installation through holes, so the heat loss at the leading surface is relatively large. Nevertheless, in non-rotational asymmetry channels, and the Nusselt number at the leading and trailing surface is quite different. What's more, the leading and trailing surfaces of the outer channel are connected by titanium alloy pin fins, the data of the outer leading and trailing surfaces cannot be used alone. Analyzed the average Nusselt number of the outer leading and trailing surfaces more accurately. Therefore, in the data provided later, there are only three data areas along the span: inner leading, inner trailing and outer averaging.

Under different Reynolds numbers, the heat transfer distribution trend of the leading and trailing surfaces of the inner and outer regions of the channel are awfully identical. The overall results

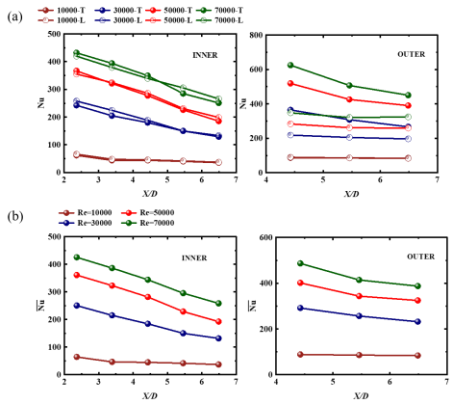

Fig. 4 Non-rotating Nusselt number of the leading and trailing edges at different Reynolds numbers

showed that the Nusselt number decreases along the flow direction due to the development of lateral outflow and thermal boundary layer. It is noteworthy that the Nusselt number at the channel inlet is significantly higher than that at other locations. On the inner smooth surface, at Re=30000, the leading and trailing averaged Nusselt number of the point near the inlet is about 48% higher than that at the end of the channel, but on the outer pin-fin arrayed surface, the averaged Nusselt number decreases about 20.5%. The cold air flows into the channel from the inlet, it is gradually heated and flows out along the lateral outlet when flowing radially outward, which inevitably leads to the reduction of the cooling efficiency of the downstream cold air, that is, the average Nusselt number decreases along the way. Moreover, the worst heat transfer occurs in the inner top corner. When the coolant flowed through the L-shaped channel, there is vortex located at the inner top corner, so the heat transfer in the region is weakened.

4.2 Heat transfer variations in the rotating channels

Before an in-depth discussing the effect of rotation on the heat transfer of lateral outflow channel, it is necessary to briefly discuss the trend observed in the rotating channel to prove the effectiveness of the channel test data. Figure 5 shows the Nusselt number trend of the leading surface and trailing surface of the inner smooth area. At rotating state, the Nusselt number of the trailing surface is higher

than that of the leading surface under different Reynolds numbers. The Coriolis force and Buoyancy caused by the rotation increased the fluid velocity near the trailing surface of the radial outflow channel. Moreover, Coriolis force and buoyancy force caused by rotation enhance the heat transfer on the trailing surface, but this enhancement is at the cost of reducing the heat transfer coefficient on the leading surface.

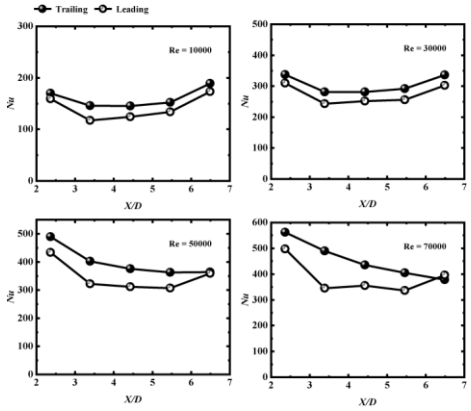

Fig. 5 Nusselt number of the leading and trailing surfaces of inner channel.

In this paper, the parameter Nusselt number ratio (Nu/Nus) is used to analyze the effect of rotation on heat transfer. The Nusselt number ratio variations of rotating channel at four Reynolds numbers are plotted in Fig. 6. It can be observed that the average Nusselt numbers of the leading and trailing edges at the high radius of the inner region are increased due to rotation. Under rotating speed is 1000 r/min condition, compared with the non-rotating state, the average Nusselt number near the end wall (P4 and P12) in the inner region increases by 4.97 times when the Reynolds number is 10000, 2.43 times when the Reynolds number is 30000, 1.88 times when the Reynolds number is 50000 and 1.5 times when the Reynolds number is 50000. With the increase of Reynolds number, the heat transfer intensity near the end wall decreases compared with the non-rotating state at the same rotating speed. The reason inferred as the increase of Reynolds number makes the cooling capacity in the channel enough. Although there is lateral outflow, the cooling capacity at the end of the channel is still strong in the non-rotating state. There is no obvious change in the enhancement of heat transfer along the radial direction in the pin fins array area of outer channel. Interestingly, with Reynolds number increases, the Nusselt number ratios decreases. When the rotating speed is 1000r / min and the Reynolds number is 10000, 3000, 50000 and 70000, the Nusselt number ratios are 2.11, 1.40, 1.19 and 1.07 respectively. Due to the increase of Reynolds number, the flow resistance in the pin fin array area increases, resulting in the decrease of Nusselt number ratio.

4.3 Effects of rotation number

The effects of rotation in high-radius and low-radius regions on heat transfer are different. It is necessary to quantitatively analyze the influence of rotation in different positions of the channel on heat transfer. Fig.7 (a) illustrates the averaged Nusselt number ratio of inner channel, Fig.7 (b) shows averaged Nusselt number ratio of outer channel. Both inner and outer of the channel, in the low Reynolds number case, the Nusselt number increases obviously with the speed； but

at

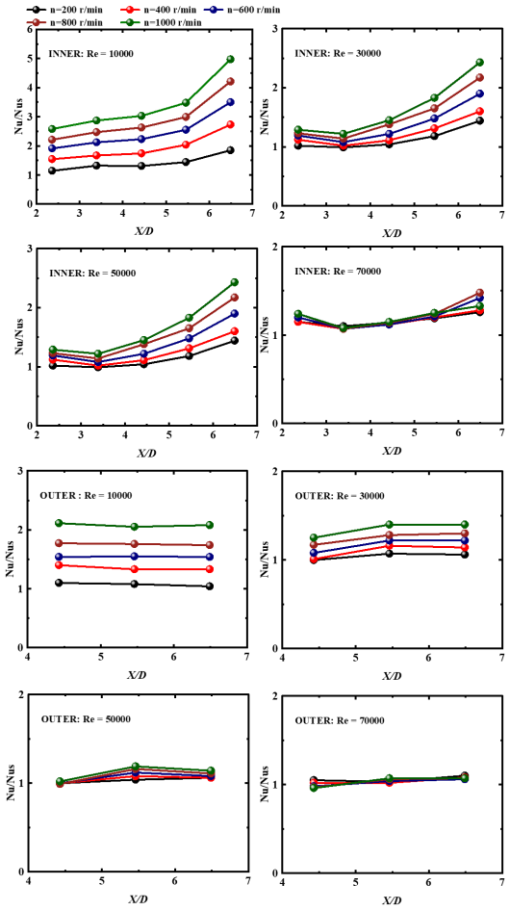

Fig. 6 Effect of rotating speed on the Nusselt number ratios

high Reynolds number case, the influence of speed on heat transfer is very limited. At the inner of the channel, the heat transfer enhancement degree at different dimensionless positions are distinct, and the heat transfer strengthened at X/D = 2.36 near the inlet of the channel is most obvious. At the position X/D = 2.36, when the Reynolds number is 10000, the speed of 1000 r/min increases 146% compared with 100 r/min, 22% when the Reynolds number is 30000, 16% when the Reynolds number is 50000 and 12% when the Reynolds number is 70000. Whereas, at the outer of the channel, there is no significant difference in the degree of heat transfer enhancement at various dimensionless location. When the Reynolds number is 70000 and the rotating speed is 200 R/min, the difference of the average Nusselt number of the outer three dimensionless points is the largest, which is 20%. When the Reynolds number is 10000 and the rotating speed is 900 r/min, the difference of the average Nusselt number of the three dimensionless points is the smallest, only 1%.

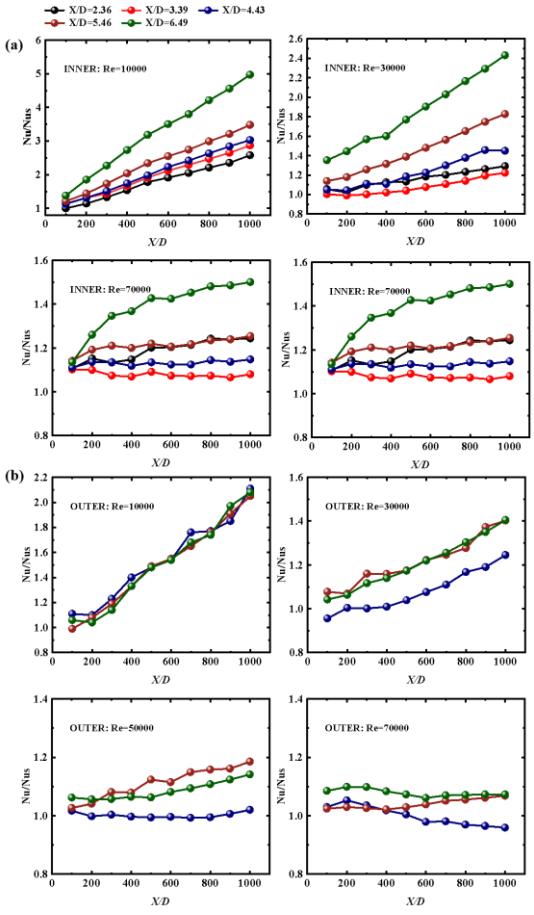

Fig. 7 The averaged Nusselt number ratio distribution on the leading and trailing surface at different locations.

Fig.8 (a) illustrates the averaged Nusselt number ratio variation of different inner trailing surface locations in radical direction, Fig.8 (b) shows averaged Nusselt number ratio variation of different

the inner leading surface locations. The Nusselt number at the trailing surface of the smooth region shows an upward trend with the increase of rotating speed. An interesting phenomenon is observed that, critical speed of the inner leading surface was found at X/D =3.39 and X/D = 4.43. The Nusselt number increases before this critical point but decreases after that. However, the critical rotation number is different at different measuring points. The critical rotating speed of X/D =3.39 is approximately 300r/min. Owing to the larger influence of the centrifugal force than that of the Coriolis force. Therefore, at small rotating speed, the Coriolis force dominates the flow, and a large amount of fluid is discharged out of the cooling channel without flowing through the entire channel. Consequently, with the increase of rotating speed, the heat exchange of the channel downstream weakened and the heat transfer at the entrance of the channel increased. With the continuous strengthening of the rotation effect, the centrifugal force becomes the dominant factor after reaching a critical number of rotations. Therefore, the fluid flows to the large-radius area, which inhibits the heat transfer of the channel at the entrance and increases the heat transfer of the large-radius area.

4.4 Effect of high Reynolds number and high rotating speed on heat transfer

The average Nusselt numbers of rotating channel at four rotating speeds are plotted in Fig. 9. With the increase of Reynolds number, the average Nusselt numbers

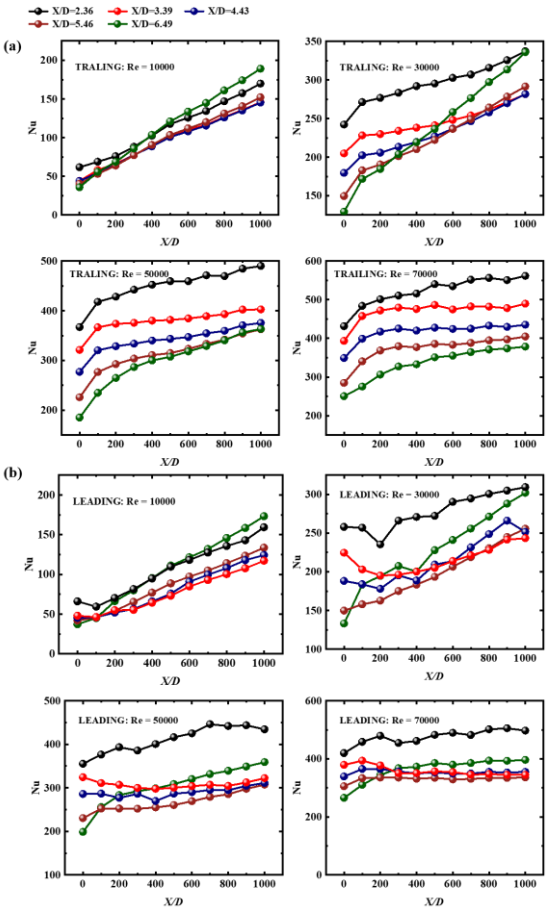

Fig. 8 The Nusselt number distribution on the inner surface at different locations.

of the inner and outer regions shows a consistent upward trend. When the rotating speed is 100r / min, the heat transfer enhancement of inner is most obvious at X/D = 3.39. The heat transfer coefficient at Reynolds number 80000 is 8.38 times that at Reynolds number 10000. The heat transfer enhancement is most obvious at X/D = 4.43 in the outer region. The heat transfer coefficient at Reynolds number 80000 is 5.33 times higher than that at Reynolds number 10000. Increasing Reynolds number is the most effective way to improve heat transfer intensity.

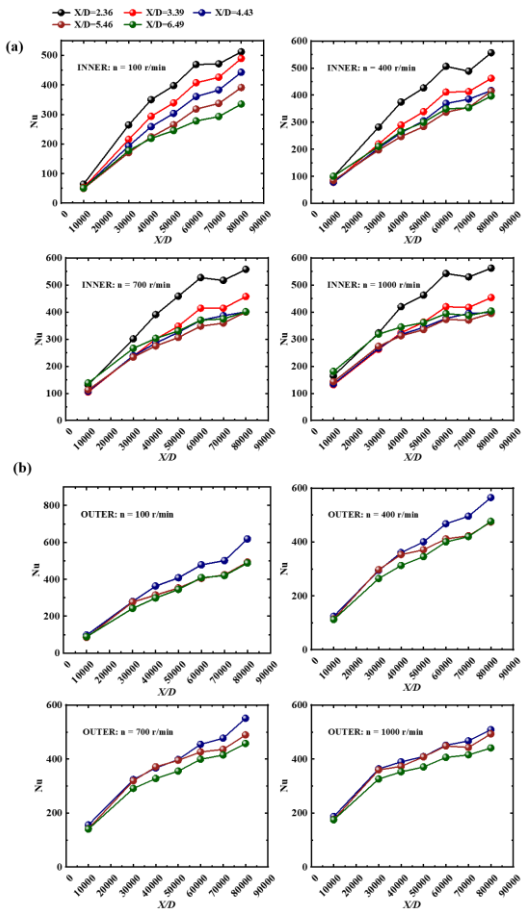

Fig. 9. the average Nusselt numbers of rotating channel at four rotating speed

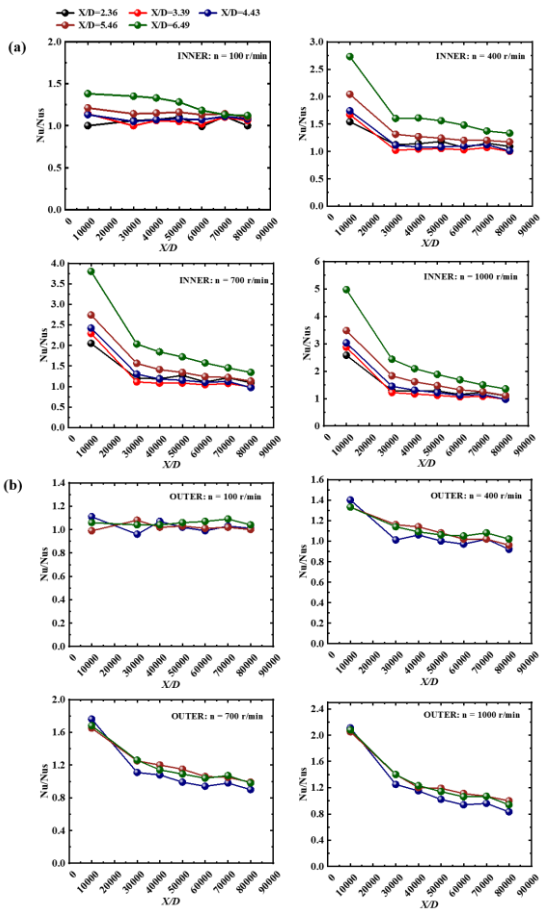

As with Fig. 10, the average Nusselt numbers ratios of rotating channel at four rotating speeds.

As with Fig. 10, the average Nusselt numbers ratios of rotating channel at four rotating speeds are plotted. As the Reynolds number increases （rotation number decreases）, the Nusselt number ratios decrease.

5. Conclusions

In this paper, the heat transfer in the internal cooling structure of aeroengine turbine rotor blade with lateral outflow pin fin trailing edge channel is studied experimentally. The heat transfer trend along the channel and the influence of Reynolds number and rotating speed on the heat transfer level are considered. Based on the above analysis, some valuable conclusions were drawn：

(1) At non-rotating state, the overall results showed that the Nusselt number decreases along the flow direction due to the development of lateral outflow and thermal boundary layer.

(2) Based on reducing the heat transfer coefficient on the leading surface, the Coriolis force and buoyancy force caused by rotation enhance the heat transfer on the trailing surface.

(3) At low Reynolds number, the Nusselt number increases obviously with the speed, but at high Reynolds number, the influence of speed on heat transfer is limited.

(4) As the Reynolds number increases

（rotation number decreases）, the Nusselt number ratios decrease.

Competing Interests

The authors do not have any conflicts of interest to declare.

Acknowledgements

Funding: This work was supported by the National Natural Science Foundation of China [grant number 51906008]; Fundamental Research Funds for the Central Universities [grant number YWF-21-BJ-J-822]; and National Science and Technology Major Project [grant number 2017-III-0003-0027]. The funding sources were not involved in study design; in the collection, analysis and interpretation of data; in the writing of the report; and in the decision to submit the article for publication.

Author Contribution

Xuejiao Zhang: Formal analysis, Investigation, Writing-original draft. Haiwang Li: Supervision, Conceptualization. Ruquan You: Conceptualization, Data curation Writing-review & editing. Song Liu: Revise, Investigation. Zhi Tao: Supervision, Conceptualization.

References

[1] Han J. C., 2018. “Advanced cooling in gas turbines 2016 max jakob memorial award paper”. *J. Heat Transf., **140*** (11).

[2] Han J. C., 2006. “Turbine blade cooling studies at Texas A&M University: 1980-2004”. *Journal of thermophysics and heat transfer, **20***(2): 161-187.

[3] Fu W. L., Wright L M Han J C. 2006. “Rotational buoyancy effects on heat transfer in five different aspect-ratio rectangular channels with smooth walls and 45degree ribbed walls”. *ASME Journal of Heat Transfer, **128***(11): 1130-1141.

[4] Li Y., Xu G., Deng H., et al. 2014. “Buoyancy effect on heat transfer in rotating smooth square U-duct at high rotation number”. *Propulsion and Power Research, **3(***3): 107-120.

[5] J.H. Wagner, B.V. Johnson, F.C. Kopper, 1991. “Heat transfer in rotating serpentine passages with smooth walls”. *J. Turbomachine. **113***(3): 321–330.

[6] Y.H. Liu, M. Huh, J.C. Han, 2012. “High rotation number effect on heat transfer in a trailing edge channel with tapered ribs”. *Int. J. Heat Fluid Flow 33*(1):182–192.

[7] Liu Y. H., Huh M., Wright L. M., et al., 2012. “Heat transfer in trailing-edge channels with slot ejection under high rotation numbers”. Journal of Thermophysics & Heat Transfer, 23(2):305-315.

[8] Hwang J. J., Lai D. Y., Tsia Y. P., 1999. “Heat transfer and pressure drop in pin-fin trapezoidal ducts”. *Journal of Turbomachinery, **121***(2).

[9] Zhi Tao, Lu Qiu, Hongwu Deng. 2015. “Heat transfer in a rotating smooth wedge-shaped channel with lateral fluid extraction”. *Applied Thermal Engineering,* 47-55.

[10] Deng H., Li L., Zhu J., et al. 2018. “Heat transfer of a rotating two-inlet trailing edge channel with lateral fluid extractions”. *International Journal of Thermal Sciences, **125***:313-323.

[11] Wright L. M., Liu Y. H., Han J. C., et al. 2008. “Heat transfer in trailing edge wedge-shaped pin-fin channels with slot ejection under high rotation numbers”. *ASME Turbo Expo 2010: Power for Land, Sea, and Air.*

[12] Metzger D. E., Fan C. S., Haley S. W., 1984. “Effects of pin shape and array orientation on heat transfer and pressure loss in pin fin arrays”. *Asme Transactions Journal of Engineering Gas Turbines & Power, **106***(1):252-257.

[13] Facchini B., Innocenti L., Tarchi L., 2004. “Pedestal and end-wall contribution in heat transfer in thin wedge-shaped trailing edge”. *ASME Turbo Expo 2004: Power for Land, Sea, and Air.*

[14] Chyu, M., Hsing, Y., and Natarajan, V., 1998. “Convective heat transfer of cubic fin arrays in a narrow channel”. *Journal of Turbomachinery*, 362–367.

[15] Hwang J. J., Lu C. C., 2001. “Lateral-flow effect on end-wall heat transfer and pressure drop in a pin-fin trapezoidal duct of various pin shapes”. *Journal of Turbomachinery, **123***(1).

[16] Ce Liang, Yu Rao, Jiahao Luo, Xiling Luo, “Experimental and numerical study of turbulent flow and heat transfer in a wedge-shaped channel with guiding pin fins for turbine blade trailing edge cooling”. International Journal of Heat and Mass Transfer, 178.

[17] Goldstein R. J., Chen S. B., 2007. “Flow and mass transfer performance in short pin-fin channels with different fin shapes”. *International Journal of Rotating Machinery, **4***(2).

[18]] O. Uzol, C. Camci, 2001. “Elliptical pin fins as an alternative to circular pin fins for gas turbine blade cooling applications: part 1–end-wall heat transfer and total pressure loss characteristics”. *ASME Turbo Expo 2001: Power for Land, Sea, and Air, American Society of Mechanical Engineers Digital Collection*.

[19] Dhumne M., 2013. “Heat transfer analysis of cylindrical perforated fins in staggered arrangement review”. *International Journal of Innovative Technology & Exploring Engineering, **5***(5S).

[20] Brigham B. A., Vanfossen G. J., 1984. “Length to diameter ratio and row number effects in short pin fin heat transfer”. *Journal of Engineering for Power, **106***(1):241-245.

[21] Pascotto M., Armellini A., Casarsa L., et al. 2012. “Effects of rotation and channel orientation on the flow field inside a trailing edge internal cooling channel.” *Asme Turbo Expo Gt.*

[22] Qiu L., Deng H., Tao Z., 2012. “Effect of channel orientation in a rotating wedge-shaped cooling channel with pin fins and ribs”. *Asme Turbo Expo: Turbine Technical Conference & Exposition.*

[23] B. Srinivasan, A., Dhamarla, C., Jayamurugan, A. B., Rajan, 2014. “Numerical studies on effect of channel orientation in a rotating smooth wedge-shaped cooling channel, American Society of Mechanical Engineers Digital Collection”. *Asme*

Turbo Expo.

[24] Willett F. T., Bergles A. E., 2001. “Heat transfer in rotating narrow rectangular ducts with heated sides oriented at 60 to the r-z Plane”. *Journal of turbomachinery,* ***123***(2): 288-295.

[25] Han J. C., Zhang Y. M., Kalkuehler K., 1993. “Uneven wall temperature effect on local heat transfer in a rotating two-pass square channel with smooth walls”. *Journal of Heat Transfer,* ***115***(4):912-920.

[26] Han J. C., Zhang Y. M., Lee C. P., 1994. “Influence of surface heating condition on local heat transfer in a rotating square channel with smooth walls and radial outward flow”. *Journal of Turbomachinery*, ***116***(1): V004T09A005.

[27] L. Bai, H. Deng, Z. Tao, et al, 2019. “Rotational effects on heat transfer in a two-inlet rectangular channel roughened with pin-fins”. *Int. J. Heat Mass Transf.,* ***143***(Nov.):118555.1-118555.10.